

Iron Based Cathode Catalyst for Alkaline Fuel Cells

Thesis

Presented in Partial Fulfillment of the Requirements for Honors Research Distinction at
The Ohio State University

By

Christopher Bruening

Undergraduate Program in Chemical Engineering

The Ohio State University

2014

Thesis Committee:

Dr. Umit Ozkan, Advisor

Dr. Kurt Koelling

Copyright by
Christopher Bruening
2014

Abstract

Alkaline fuel cells take advantage of the reaction between hydrogen and oxygen to produce water and an electrical current. During the reaction, a hydroxide ion passes through a membrane from the oxygen side cathode to the hydrogen side anode. Previous research had been conducted on synthesis and evaluation of iron based catalysts for PEM fuel cells by the Heterogeneous Catalysis Research Group at The Ohio State University. PEM fuel cells use a similar reaction between hydrogen and oxygen except a proton travels across the membrane from the hydrogen side to the oxygen side, so the reaction mechanism differs. This paper looks into those same iron based catalysts tested in an alkaline environment. The catalyst in particular is 1% iron in 1:1 Black Pearls 2000 : 1,10 phenanthroline. Those precursors are combined using a wet impregnation and then the result is ball milled. It then undergoes an argon pyrolysis at 1050°C and an ammonia pyrolysis at 950°C which are the final steps in the synthesis. The completed catalyst can then be washed in acid for 1 hour, 2 days, or 1 week to compare the effect of acid washing on different factors. The different catalysts are compared at each stage in the synthesis mainly by their onset potential, which is the voltage where it produces a current density of 0.1 mA/cm². Another method of comparison is the selectivity of a catalyst towards the main reaction vs a side reaction that produces hydrogen peroxide. It was found that this catalyst performed comparably with platinum for both onset potential and selectivity. Another finding was that the acid washing did not have a very significant effect on either.

Acknowledgments

Help from former OSU graduate student Deepika Singh, current graduate student Kuldeep Mamtani, Dr. Umit Ozkan, and the Heterogeneous Catalysis Research Group is gratefully acknowledged.

Vita

May 2010 Tippecanoe High School
Summer 2010 Air Force Research Lab Sensors Directorate, Engineering Intern
Summer 2011 Air Force Research Lab Materials Directorate, Engineering Intern
Summer 2012 Anomatic Corporation, Assembly Co-Op
Jan-August 2013..... Anomatic Corporation, Anodizing Co-Op

Fields of Study

Major Field: Chemical and Biomolecular Engineering

Table of Contents

| | |
|---|-----|
| Abstract | ii |
| Acknowledgments | iii |
| Vita | iv |
| List of Figures | vi |
| Chapter 1: Introduction | 1 |
| Chapter 2: Methodology | 3 |
| Chapter 3: Results and Discussion | 11 |
| Chapter 4: Conclusions | 20 |
| References | 21 |
| Appendix | 22 |

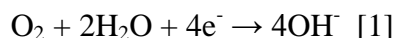
List of Figures

| | |
|--|----|
| Figure 1: Current vs Disk Potential for scan in alkaline medium | 8 |
| Figure 2: Current vs Disk Potential for scan in alkaline medium with argon scan subtracted out | 9 |
| Figure 3: Current Density vs Potential for typical scans on various catalyst types | 12 |
| Figure 4: Comparison of onset potential of platinum to iron catalysts in alkaline environment | 14 |
| Figure 5: Comparison of selectivity of platinum to iron catalysts in alkaline environment at 1600 rpm and 0.5 V | 16 |
| Figure 6: Current Density vs Potential durability scan for platinum catalyst | 17 |
| Figure 7: Current Density vs Potential durability scan for ball milled and argon treated catalyst..... | 18 |
| Figure 8: Current Density vs Potential durability scan for ball milled, argon treated, and ammonia treated catalyst..... | 18 |
| Figure 9: Current Density vs Potential durability scan for ball milled, argon treated, ammonia treated, and acid washed catalyst | 19 |
| Figure 10: Diagram of RRDE and half-cell reaction | 12 |
| Figure 11: Pyrolysis furnace with quartz tube sitting in front | 23 |
| Figure 12: RRDE setup with acid container, reference electrode (back left), counter electrode (front left), and gas diffusor (front right) | 23 |
| Figure 13: Current Density vs Potential at different disk rotational speeds | 24 |
| Figure 14: Current Density vs time at different platinum ring rotational speeds | 25 |

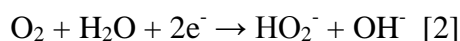
Chapter 1: Introduction

Alkaline fuel cells use the reaction between hydrogen and oxygen forming water to generate an electrical current. Hydroxide ions travel across a membrane while electrons travel through a loop to complete the reaction. Alkaline fuel cells have been used in a practical manner by NASA during the Apollo moon landing program (Olson et al, 5049). Alkaline fuel cells are used in spacecraft systems to both generate usable water and electricity from the reaction. One reason why they have not been put into use on the Earth's surface is due to the ease at which they become poisoned. Carbon dioxide poisons an alkaline fuel cell very easily so the oxygen source cannot be from air as it is with PEM fuel cells. The incoming oxygen and hydrogen must be very pure which leads to high cost. This cost as well as the cost of the catalyst itself is not as important in an area such as space exploration since it is minimal compared to other costs associated with launching large payloads into orbit. Durability is also an area that needs to be improved for alkaline fuel cells so that they can perform for a longer amount of time (energy.gov).

The main reaction in an alkaline fuel cells concerns hydrogen and oxygen, but for the purpose of testing catalysts, a half cell reaction is considered. The oxygen reduction side of the reaction in which oxygen is reduced to hydroxide is the main reaction taking place and is as shown in equation [1]. This reaction has an electrochemical potential of 0.236 V vs. Hg/HgO in 0.1 M sodium hydroxide solution (Chen et al, 20689).



An alternate reaction that occurs in an alkaline fuel cell is the formation of hydrogen peroxide. The oxygen reduction side of this reaction is shown in equation [2] and produces hydroperoxyl which is undesirable. Not only is hydrogen peroxide harmful, but the electrochemical potential of the half reaction is -0.230 V vs. Hg/HgO in 0.1 M sodium hydroxide solution (Chen et al, 20689). Therefore, the selectivity of the catalyst towards the first reaction is of high importance.



A specific iron based catalyst that had been extensively tested for PEM fuel cells by the Heterogeneous Catalysis Research Group was considered for experimenting in an alkaline medium. PEM fuel cells use a similar reaction to alkaline fuel cells, but instead of hydroxide, a proton travels across the membrane to complete the reaction. Since the mechanism differs, it is useful to know how this catalyst performs in an alkaline environment versus an acidic environment.

Chapter 2: Methodology

Current non-noble metal catalysts generally use iron or cobalt along with a nitrogen precursor and a carbon support (Jaouen, Frederic et al 114). The previously tested iron based catalysts in an acidic environment were to be tested in an alkaline environment. The catalysts were created by performing a wet impregnation of Iron Acetate with Black Pearls 2000 (BP) and 1,10 phenanthroline (Ph) to create a catalyst that was 1% by weight Fe in 1:1 BP:Ph. 500 mg of Ph was added to a beaker with 100 mL of DI water and 50 mL of 200 proof ethanol. Then 31.146 mg of iron acetate and 500 mg of BP was added to the beaker. Finally the beaker is partially covered, placed in a water bath on a heater stirrer set at 70°C, and let to sit until about 2/3 of the mixture has evaporated off. Then it is transferred to an oven set at 90°C and let to sit overnight to create a powder. The dried catalyst then underwent ball milling at 200 rpm for three hours. After the catalyst was placed into the ball mill jar with chrome grinding balls, it was placed into a glove bag where nitrogen was allowed to fill the environment before capping the jar. This is done so that there is no reaction taking place during the milling. The ball milling opens up available area of the catalyst.

Then heat treatment steps in both argon and ammonia environments took place. The argon pyrolysis was at 1050 °C for 1 hour. For the pyrolysis steps, the catalyst was placed into a quartz tray and then the tray was placed into the furnace tube that was plugged on both ends and was configured to allow certain gasses to flow through. A

picture of this setup can be found in Figure 11. The tube was placed into the furnace and argon was flowed for around 10 minutes. At this point, the quartz tray was in the tube but in a section that is outside of the furnace. Then the heat was ramped up at 15 °C until it reached the desired temperature and then the tray was moved into the furnace section. After the hour, the furnace was opened and the tube was removed and set on bricks for cooling with argon flowing the entire time. Once cooled, the tray was removed and the catalyst could be stored in a vial. For the ammonia pyrolysis, the same setup procedure was used and Argon is still flowed until the furnace reached 950 °C. Once this temperature was reached, an ammonia flow was switched on as well as the argon switched off. The tray still sits outside of the furnace with ammonia flowing for around 15 minutes before it was moved into the furnace for 20 minutes. After this time, the tube was again removed for cooling and the catalyst stored. Ammonia was switched off and argon was switched back on prior to the tube being removed from the furnace.

The next step for some of the catalysts was acid washing. This is done in order to strip iron out of the support. The catalyst is transferred into a round bottom flask with about 250 mL of 1 M HCL and a stir bar. The temperature of a water bath in which the flask is inside of is held constant at 60°C through a heating plate underneath which also controls the spinning of the rod. The top of the glassware is covered and it is let to run for the specified time of 1 hour, 2 days, or 1 week. After the allotted time in the acid, the solution is vacuum filtered with a flask connected to a water spout. At least 1.5 L of

distilled water is used in the filter to remove any remaining acid. Then the catalyst is dried at 90 °C overnight and then stored in a vial for later testing.

In order to test the oxygen reduction reaction activities of catalysts, a rotating ring disk electrode (RRDE) setup has been used. A diagram of the RRDE can be seen in Figure 10. An ink is prepared with 5 mg of the catalyst in 175 mL of ethanol and 48 mL of nafion. This mixture is sonicated in an ice bath for at least an hour in order to create the ink. It is then applied to the glassy carbon disk portion of the RRDE using a micropipette and allowed to dry. 9 μ L of the ink is used for this step. Then, a bubble of distilled water is put on top of the disk and removed by touching it with a kimwipe. This is repeated 3-5 times in order to break the surface tension of the catalyst on the disk. The disk is then submerged into a specially made Plexiglas cylindrical container shown in Figure 12 which holds 0.1 M potassium hydroxide. There is also an Ag/AgCl reference electrode in the acid container which produces a potential that the main reaction can be compared against. The reference electrode is occasionally measured in the solution saturated in hydrogen in order to ensure that it hasn't changed significantly. Finally, there is a counter electrode placed into the solution in order to allow an electron flow through the circuit. For these experiments, a platinum coil with a glass shell is used as this counter electrode. At the end of the shell is a filter that allows the acid and electrons to pass through while keeping out contaminants. A disk channel, a ring channel, the reference electrode, and the counter electrode are all connected to a BioLogic USA BiStat

which communicates with the computer software to run the experiments. The computer program used is EC-Lab V10.11.

Oxygen is allowed to flow into the solution using a diffuser for 20-30 minutes before any scans begin in order to ensure saturation. The disk then rotates which allows oxygen to come into contact with the catalyst more easily. The disk typically rotates at speeds typically ranging from 0 rpm to 2500 rpm. The first scans that are run are fast scans that electrically clean the system. For the disk portion, the program scans from 0.2 V to -0.8 V and then back to 0.2 V at a rate of 50 mV/s and records the current at each potential. A disk speed of 1000 rpm is used during all fast scans. Typically three fast scans are performed in oxygen with 6 cycles per scan. Then the fast scans are performed on the ring portion. The program scans from 0.3 V to -0.1 V and then back at a rate of 100 mV/s and again records the current at each potential. This ring scan is typically performed twice in oxygen. For both fast scans it is desired that each cycle perfectly replicates the last and the scans have stabilized when this happens. If this does not happen during the pre-determined number of scans, more are done until stabilization occurs.

After the fast scans, the experimental scans in oxygen can be performed. These scans again go from 0.2 V to -0.8 V and back but at a rate of 10 mV/s and there is only one cycle per scan. These scans are performed at 0, 400, 800, 1000, 1200, 1600 and 2000 rpm. Each scan should overlap in the higher potential region of the plot because onset

potential is not a function of rotation speed. If a scan does not match the rest in this region, it is repeated. However, if too many repeat scans are performed than the activity of the catalyst can be weakened. At lower potentials, higher scan speeds produce larger currents and a comparison of scans at different rotation speeds showing this can be found in Figure 13. During these scans, the ring portion is held at a constant potential of 0.5 V while the current being produced from it is measured. Ring scan shapes can vary, but a typical one can be found in Figure 14 and they are plotted as current vs time.

Scans with argon are also performed in order to subtract out the background current produced. After the oxygen scans, the oxygen flow is switched off and argon is allowed to flow for at least 15 minutes. The same fast scans as in oxygen at 1000 rpm and 50 mV/s are repeated but it only needs to be performed twice as the readings stabilize more quickly. There are also fast scans on the ring at 1000 rpm and this is only performed once prior to the argon scans. Then the scan at 1000 rpm and 10 mV/s is performed and if this scan matches the oxygen scans in the low potential region of the plot, the experiment is complete. Many times this scan does not match and a scan at 0 rpm is performed which usually solves the problem when it occurs. Figure 1 shows a typical oxygen scan along with its matching argon scan. It shows that they overlap well in the high potential regions but then diverge as the oxygen scan sees a significant current. Figure 2 shows what the oxygen scan looks like after the argon scan is subtracted out. In the high potential region where they overlapped, the oxygen scan is at 0 mA on the scale which is necessary to determine current produced.

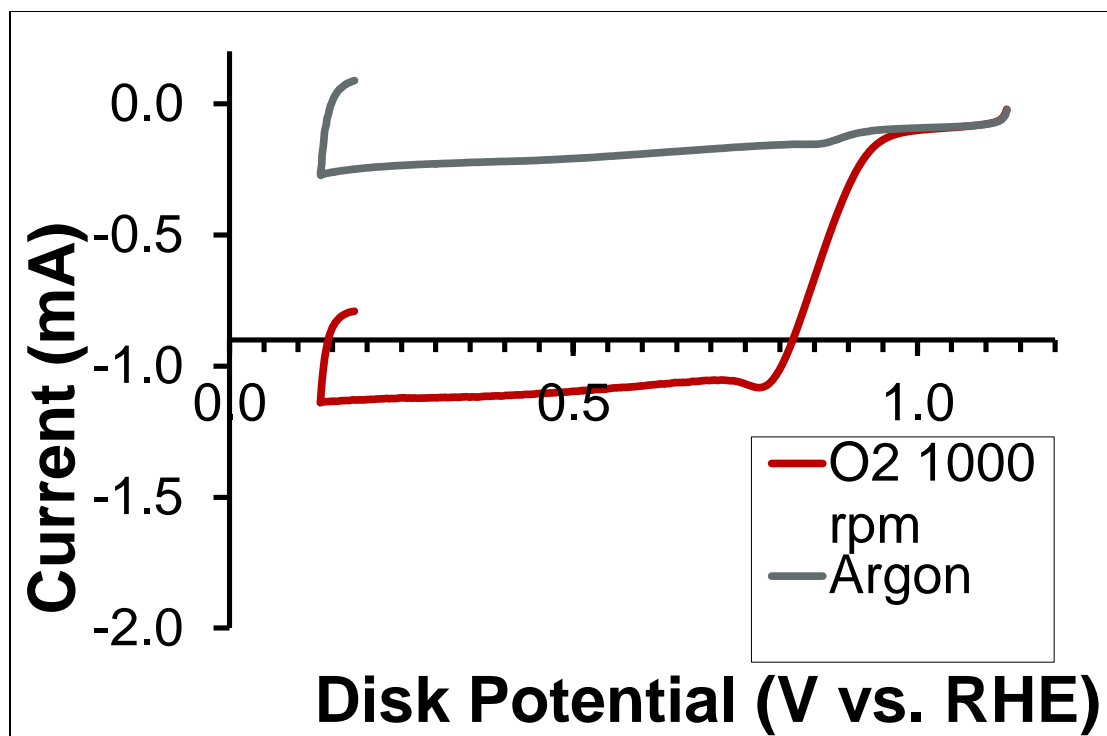


Figure 1: Current vs Disk Potential for 1000 rpm and argon scans in alkaline medium

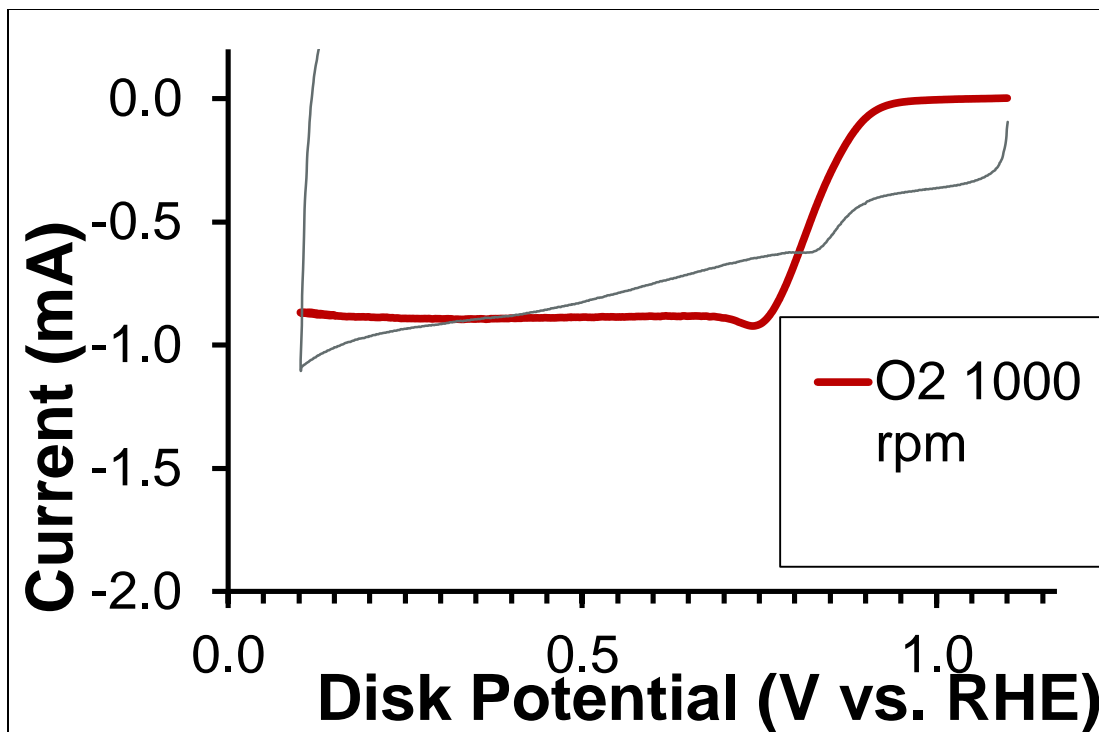


Figure 2: Current vs Disk Potential for scan in alkaline medium with argon scan subtracted out

The ring scans are used to measure the selectivity of the catalyst that occurs from the overall undesired side reaction that occurs is the formation of hydrogen peroxide. In the half cell, of course, there is only the reduction side of the reaction which was shown in equation [2]. Again, the thermodynamic potential created by this alternate reaction is much lower than that of water formation. In order to determine how much hydroperoxyl is created, there is a platinum ring portion surrounding the disk which will further reduce

the hydroperoxyl into hydroxide. It can then be calculated how much hydrogen peroxide would be created vs. the creation of water in an actual alkaline fuel cell. The other indicator of how well a catalyst performs is the onset potential. This is the potential where the current generated due to oxygen reduction becomes significantly measurable and is usually calculated in terms of current density. For all data in this report, a current density of 0.1 mA/cm² was used to determine the corresponding onset potential for a particular catalyst.

Finally, the last experiments that are performed using the RRDE are for durability. In these experiments, scans are cycled many times in order to look at the degradation of onset potential over time. The focus is on the disk and ring scans are not collected. Fast disk scans are performed the same as before as well as normal scans at 0, 400, 800, 1000, 1200, 1600 and 2000 rpm and an argon scan. Then, the argon is switched off and the oxygen switched back on for a fast scan which is performed where the BiStat scans from 0.2 V to -0.8 V and back at a speed of 100 mV/s. This scan is cycled 100 times in a row and then normal scans at 0, 1000, and 1600 rpm are collected and the new onset potential is recorded. The 100 mV/s scan is then repeated and cycled 400 times for a total of 500 cycles. Again, normal scans at 0, 1000, and 1600 rpm are collected after this cycling. After cycling, the onset potential will drop and the voltage amount that a certain catalyst drops by can be compared against other catalysts to see which ones are more durable.

Chapter 3: Results and Discussion

Figure 3 shows comparisons of Potential vs. Current Density for a typical argon treated catalyst, an argon+ammonia treated catalyst, and argon+ammonia+acid wash treated catalysts. This plot contains data that already subtracted out the background scans, and therefore the data from the different trials can be compared. From this plot, it appears that the argon-only treated catalyst is the only one that stands out and has a different onset potential than the rest. Onset potential is being defined as the voltage at which there is a current density of 0.1 mA/cm^2 above the background. Therefore, a catalyst with a higher onset potential will have a line further to the right on a graph compared to catalysts with lower onset potentials.

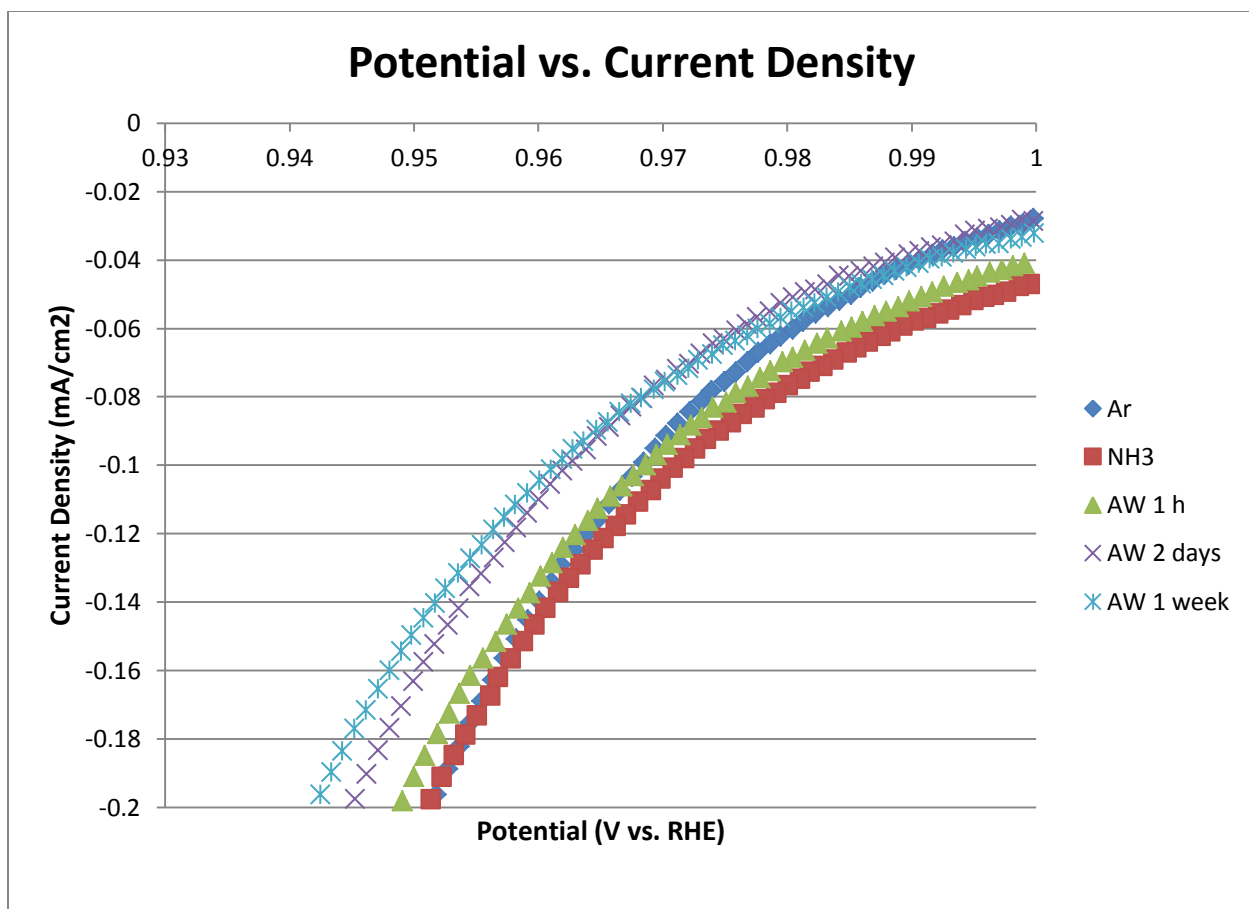


Figure 3: Current Density vs Potential for typical scans on various catalyst types

Figure 4 compares the onset potentials of the best performing catalyst of each treatment type as well as platinum. Interestingly, all treatments except for ball milled only were comparable with platinum. Also, there did not appear to be any significant activity loss from acid washing. The acid washing strips Iron from the catalyst and causes losses in an acidic environment. In the alkaline environment, the catalyst that was

acid washed for 1 day retained most of its activity and the same applied for the catalyst washed for 1 week. This implies that the active site of this catalyst is different for the reduction reaction in an acidic environment vs an alkaline environment. Since the removal of Iron isn't affecting much, the Iron may not play as large of a role as the carbon support. However, an additional onset potential of 0.84 was recorded for a catalyst that contained no iron, but was only the ball milled support with an argon pyrolysis. Since this is much lower than the same treatment but with iron, it shows that the iron and the support work together to create an active site.

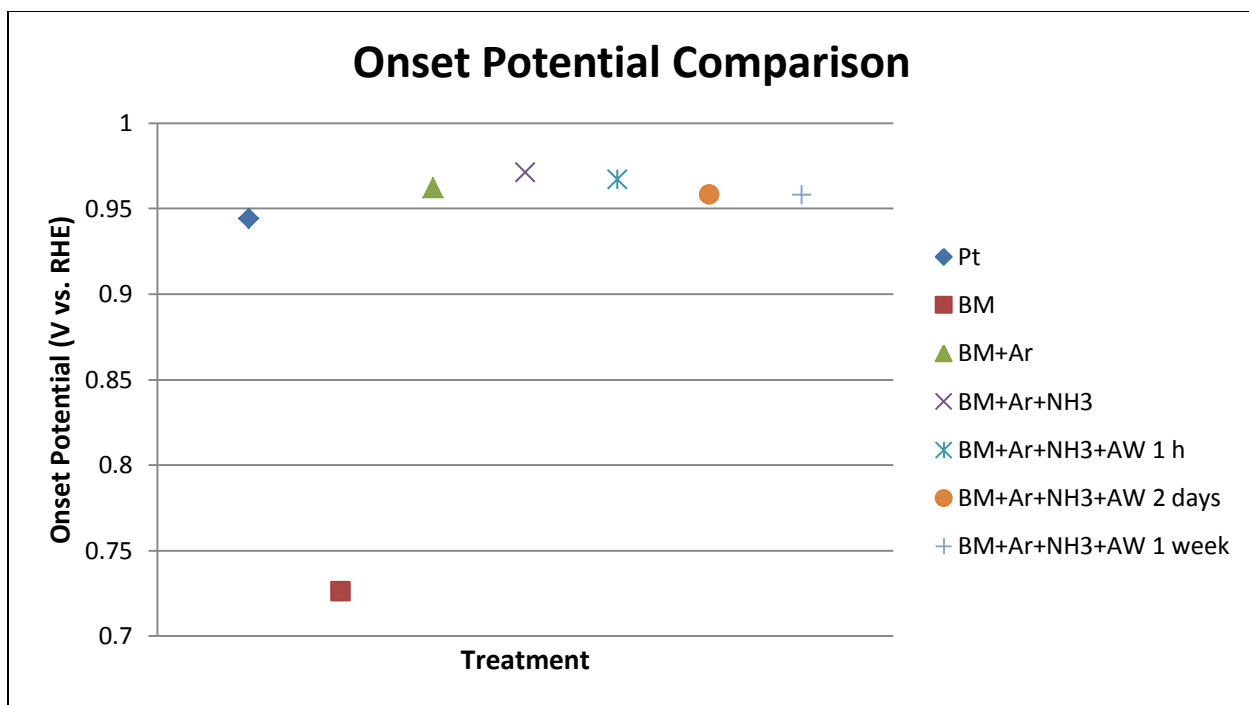


Figure 4: Comparison of onset potential of platinum to iron catalysts in alkaline environment

Figure 5 shows a similar comparison between catalysts, but with regard to selectivity. These selectivity values for each sample are associated with the same catalyst shown in the previous Figure 4 and not necessarily the catalyst with the highest selectivity. The selectivity values differ slightly between RRDE rotation speeds due to random variability, so the selectivity values are all for the 1600 rpm scan when the disk was at 0.5 V for consistency. The units for selectivity are number of electrons transferred per oxygen molecule, so a higher number indicates higher selectivity towards the main

reaction and is desired. Interestingly, the catalyst that was treated with argon and ammonia was less selective than the catalyst that was only treated with ammonia despite having a higher onset potential. The 1 h acid washed catalyst continued the downward trend while the catalysts washed for 2 days and 1 week were both higher. Overall, all the catalysts except for the ball milled only catalyst were fairly comparable to platinum.

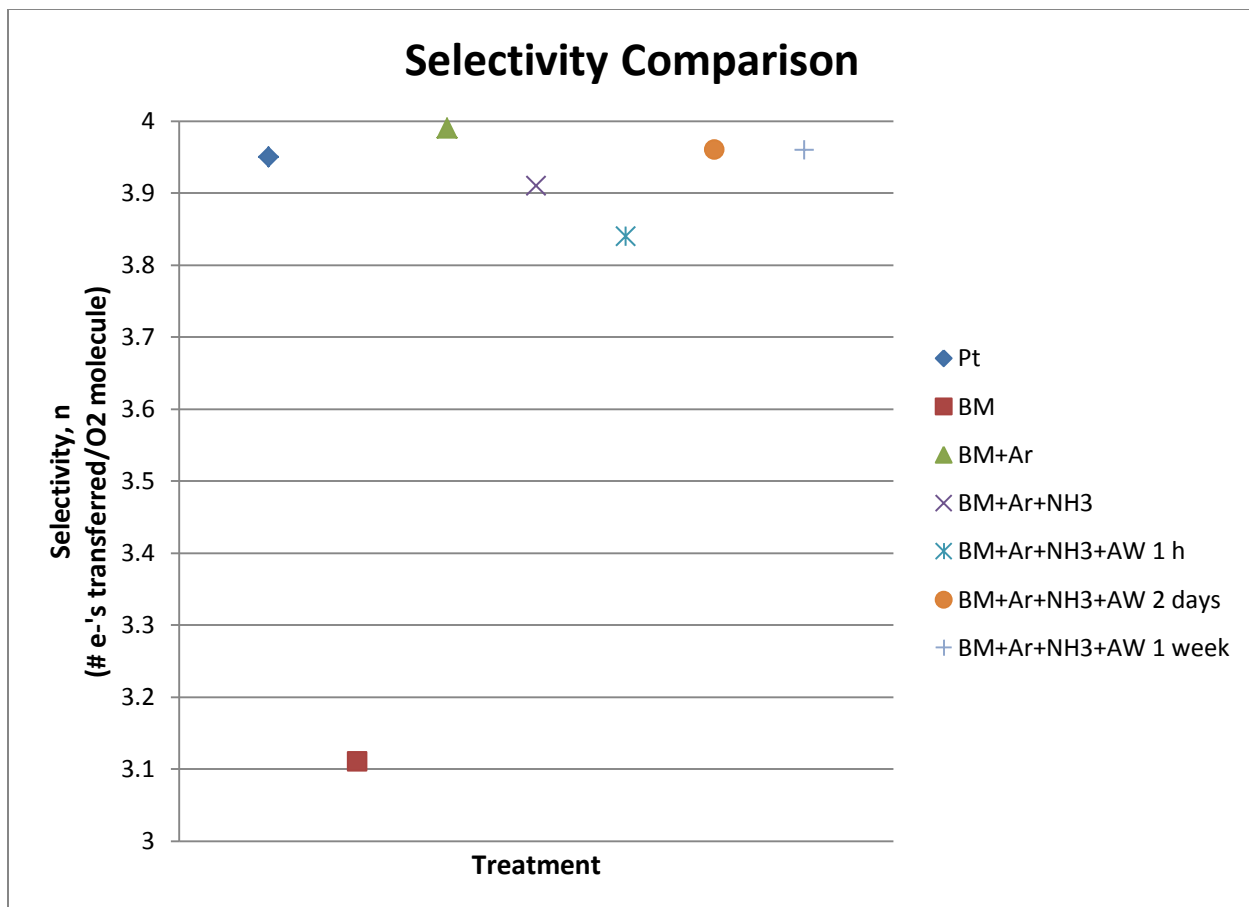


Figure 5: Comparison of selectivity of platinum to iron catalysts in alkaline environment at 1600 rpm and 0.5 V

Data for the durability testing of the platinum catalyst is available in Figure 6. There appears to be a large amount of activity loss after 100 and 500 cycles. Figures 7 and 8 show the stability testing data for ball milled plus argon pyrolysis and ball milled plus argon pyrolysis plus ammonia pyrolysis respectively. These two catalysts appear to

hold up very well. Neither has noticeable activity loss after 100 or 500 cycles. Finally, Figure 9 shows this stability testing data for a catalyst that was acid washed for one hour. This one does have activity loss after the cycles so acid washing does have an effect on the stability of the catalyst in an alkaline environment.

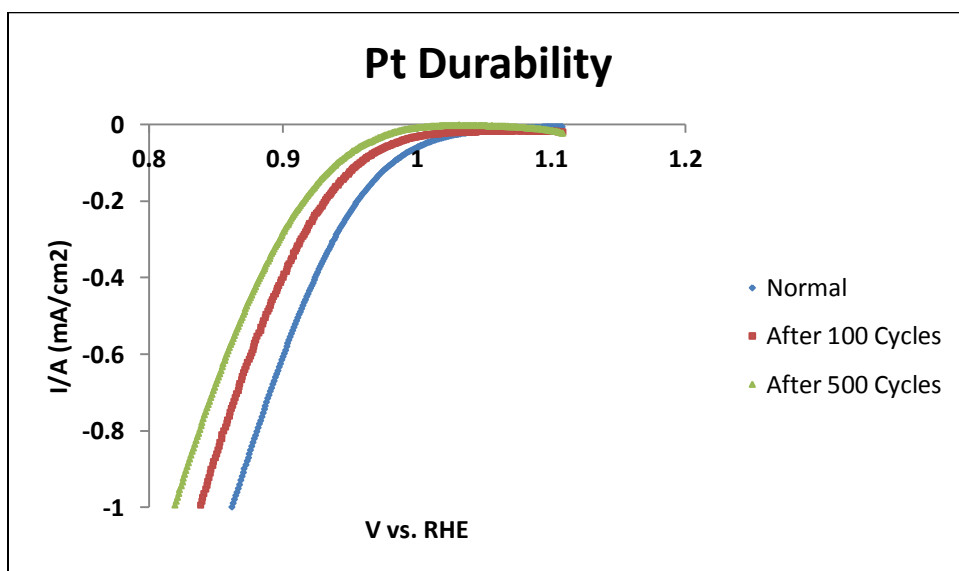


Figure 6: Current Density vs Potential durability scan for platinum catalyst

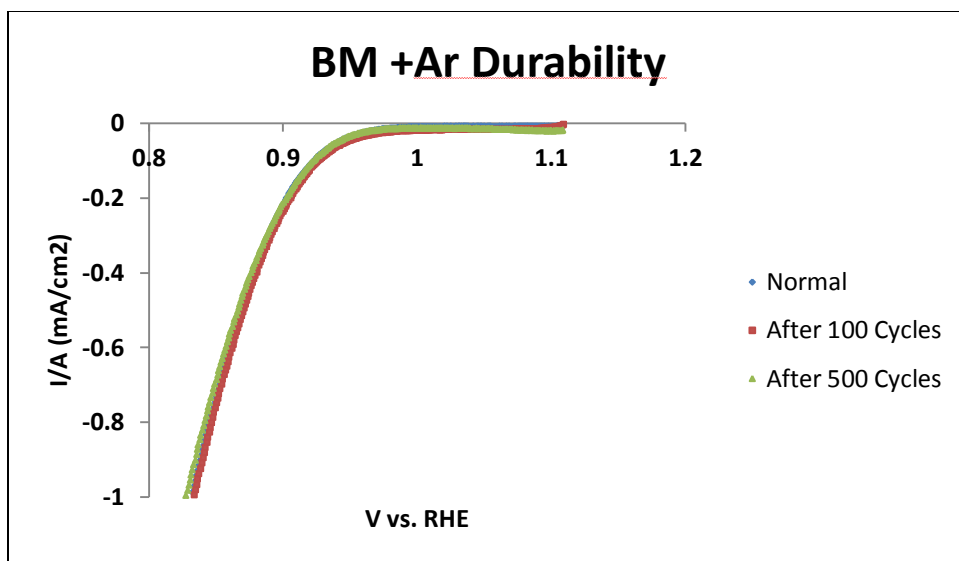


Figure 7: Current Density vs Potential durability scan for ball milled and argon treated catalyst

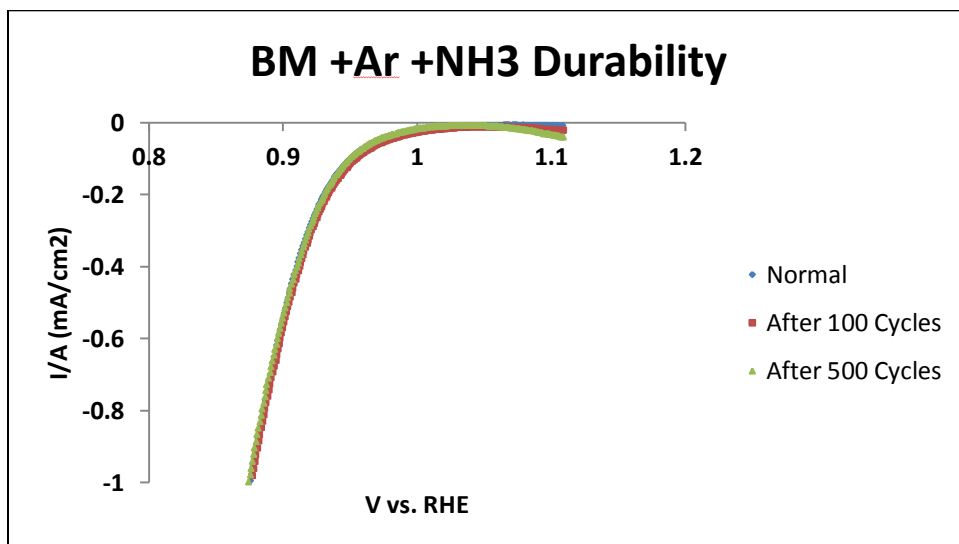


Figure 8: Current Density vs Potential durability scan for ball milled, argon treated, and ammonia treated catalyst

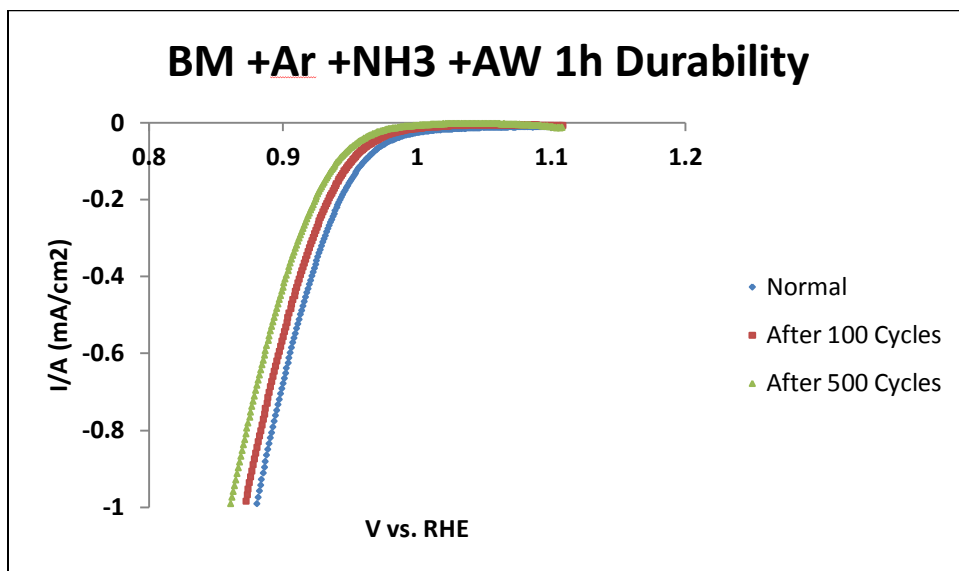


Figure 9: Current Density vs Potential durability scan for ball milled, argon treated, ammonia treated, and acid washed catalyst

Chapter 4: Conclusions

The 1% iron catalyst in 1:1 BP:Ph was found to have comparable activity and selectivity values after it was ball milled and then treated in both argon pyrolysis as well as an argon/ammonia pyrolysis combination. The catalyst that was only ball milled did not show very high activity or selectivity. In addition to these results, acid washing of the catalyst did not have significant degradation effects on either the activity or selectivity and the catalyst retained almost all of its activity after even 1 week of acid washing. This could imply that iron does not play as important of a role in being the active site, but helps to stabilize the structure of the active site during synthesis. Finally, the catalysts that underwent both pyrolysis treatments showed minimal degradation over time during tests in which they were cycled through scans up to 500 times which means that they outperformed platinum in this aspect. The tested acid washed catalyst did begin to show decrease in activity after the cycling.

References

- "Types of Fuel Cells." Energy.gov Office of Energy Efficiency & Renewable Energy. Energy.gov. Web. 15 Nov. 2014. <<http://energy.gov/eere/fuelcells/types-fuel-cells>>.
- Olson, Tim S., Et Al. "Anion-Exchange Membrane Fuel Cells: Dual-Site Mechanism of Oxygen Reduction Reaction in Alkaline Media on Cobalt-Polypyrrole Electrocatalysts." *The Journal of Physical Chemistry C* 114.11 (2010): 5049-059. PDF.
- Chen, Rongrong, Haixia Li, Deryn Chu, and Guofeng Wang. "Unraveling Oxygen Reduction Reaction Mechanisms on Carbon-Supported Fe-Phthalocyanine and Co-Phthalocyanine Catalysts in Alkaline Solutions." *The Journal of Physical Chemistry C* 113.48 (2009): 20689-0697. PDF.
- Jaouen, Frederic et al. "Recent advances in non-precious metal catalysis for oxygen-reduction reaction in polymer electrolyte fuel cells." *Energy and Environmental Science* 4.1 (2011): 114-130. PDF.

Appendix

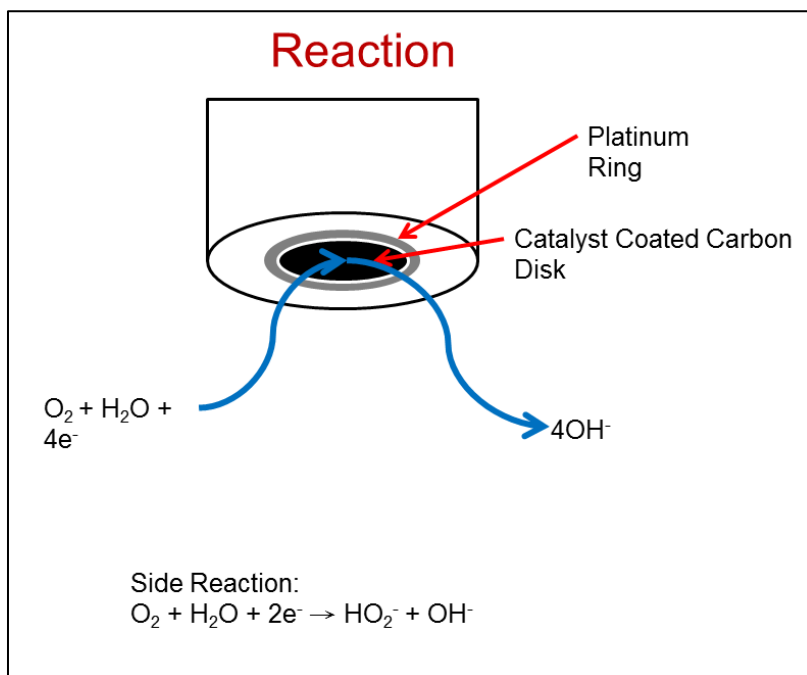


Figure 10: Diagram of RRDE and half-cell reaction



Figure 11: Pyrolysis furnace with quartz tube sitting in front

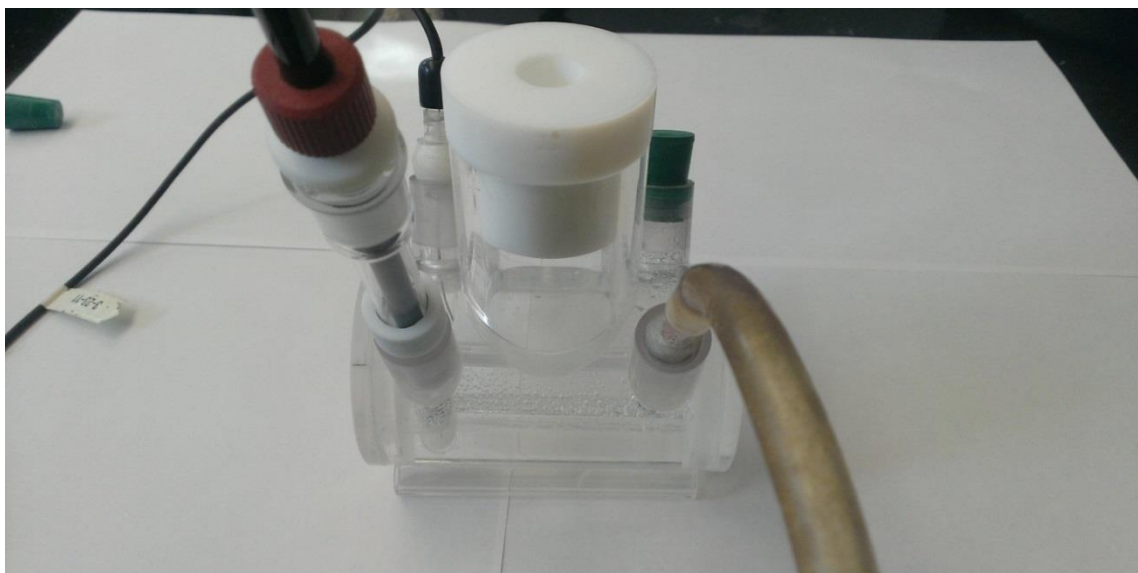


Figure 12: RRDE setup with acid container, reference electrode (back left), counter electrode (front left), and gas diffuser (front right)

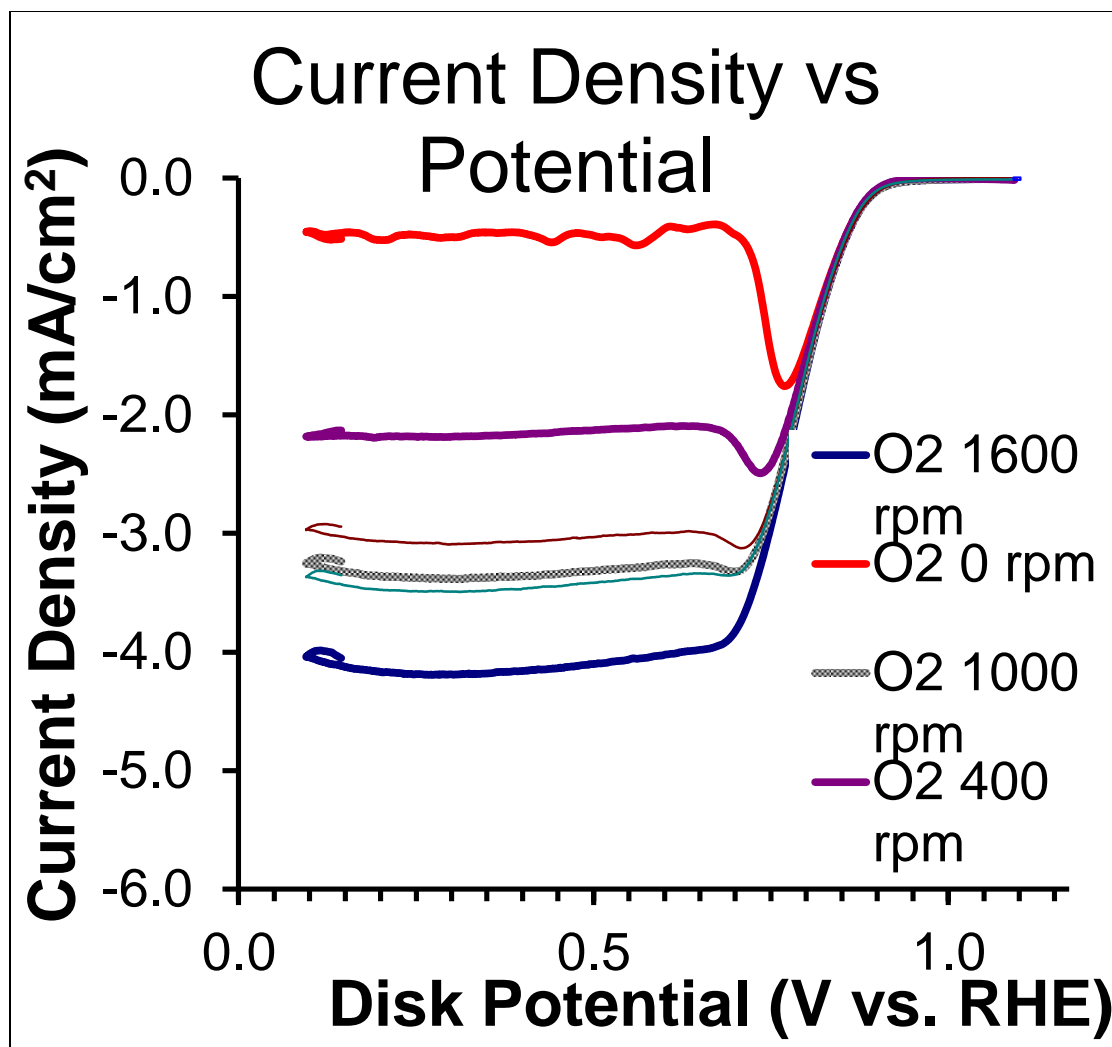


Figure 13: Current Density vs Potential at different disk rotational speeds

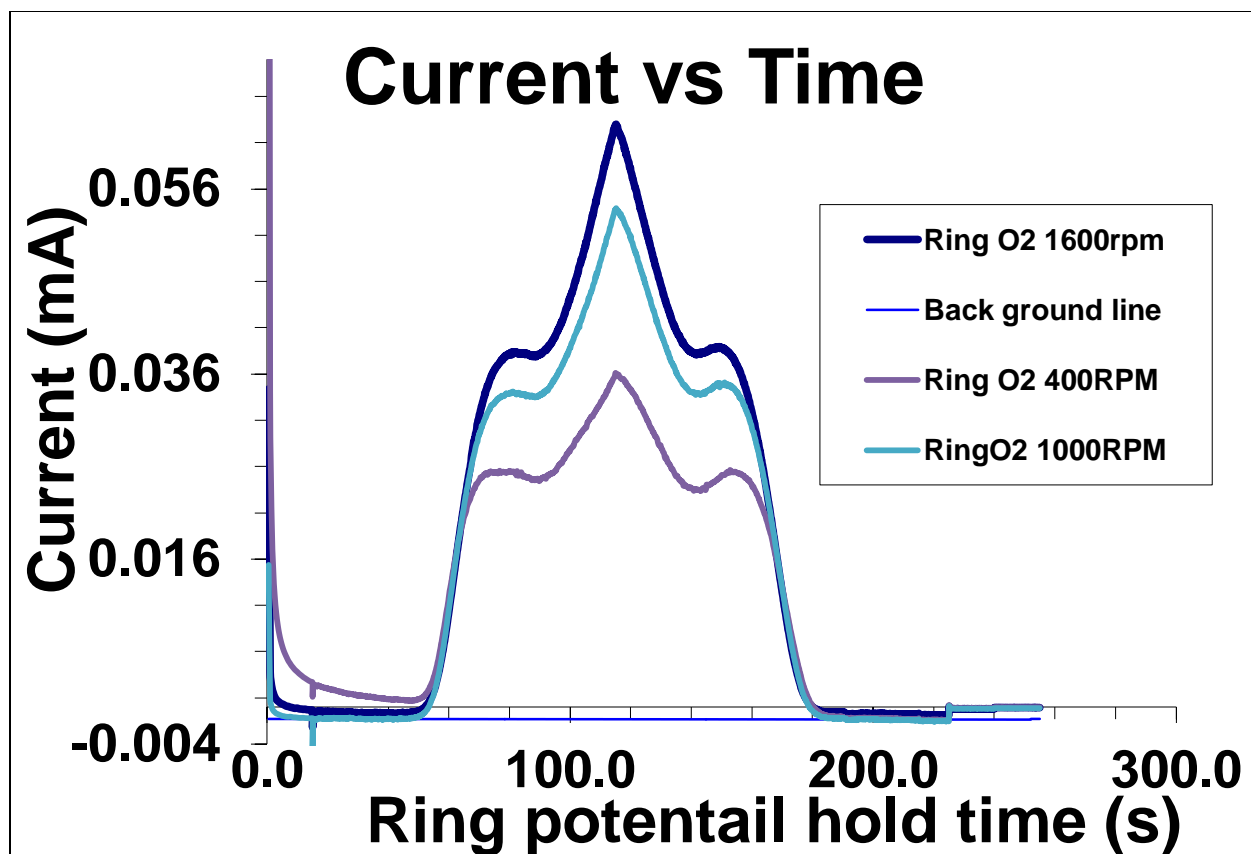


Figure 14: Current Density vs time at different platinum ring rotational speeds